


S.F. HO 
B.K.A. NGOI

Sub-microdrilling with ultrafast pulse laser interference

Precision Engineering & Nanotechnology Centre, Nanyang Technological University,
N3-B4c-03, 50 Nanyang Avenue, Singapore 639798

Received: 13 August 2003/Revised version: 24 February 2004
Published online: 28 April 2004 • © Springer-Verlag 2004

ABSTRACT A novel sub-microdrilling technique utilising the phenomenon of ultrafast pulse laser interference is reported. This technique overcomes the feature size limit of conventional laser micromachining. The method of first interfering with the laser light, and then using the central bright fringe of the interfered beam to machine has been proven to effectively reduce the effective ablation spot size and, subsequently, to reduce the size of the drilled features. Preliminary results show a 300% reduction in drilled feature size with the interfered laser beam compared with the conventional non-interfered laser beam. 300 nm holes were successfully drilled on a 1000 Å thick Gold film using the interfered laser beam compared to 1 µm holes ablated using the conventional non-interfered laser beam at the same pulse energy.

PACS 42.62.Cf; 42.15.Eq; 42.25.Hz

1 Introduction

Micro-drilling is the enabling technology for several important manufacturing processes. A very important application is in the drilling of microvias in printed circuit boards/printed wire boards (PCB/PWB) and IC packaging industries. Currently, laser-drilled vias range from 100 to 200 µm in diameter, with some speciality items requiring vias down to 25 µm in diameter [1].

Another important application is in the manufacturing of microscale fluidic devices. Among the most widely known applications is the production of ink-jet printer nozzles. This family of products also includes drug-delivery systems, micro heat-pipes and heat exchangers, fuel injectors, chemical-reactor networks, and chemical-analysis tools. Precise control of small quantities of fluid is important for all these devices, and depending on the working fluid and desired flow rates, drill hole diameters ranging from 100 µm to less than 1 µm are required [2, 3].

However, the rising trend towards miniaturisation has led to the demand for even smaller and finer drilling capabilities. For example, miniaturisation in portable electronics devices

calls for smaller high-density interconnects (HDI) for packaging and printed circuit boards. Driven by high I/O chips, the number of interconnects per layer continually rises resulting in the demand for smaller and finer vias. Currently, the number of microvias exceeds 10 000 per substrate but with the continued growth of silicon chip capabilities, this requirement will be upwards of 40 000 to 80 000 microvias per substrate in the near future [4].

Therefore, there is a need for laser-drilling technology that can produce fine holes into the sub-micron ranges with high aspect ratios and good reproducibility.

1.1 Mechanism of sub-spot size ablation with ultrafast lasers

Ultrafast pulse laser machining represents a major advancement in precision machining technology. With the advent of ultrafast pulse lasers, ablation features of sub-spot of high precision and exceptional machining quality can now be achieved, dethroning the previous notions that the minimum achievable ablation feature is limited to the laser wavelength [5, 6].

Because the threshold value of ultrafast pulse lasers can be precisely determined, in contrast to the broad threshold bandwidth of long pulse lasers, they are able to produce features substantially below that of the wavelength of the laser pulse itself. The ultrafast laser pulse has a Gaussian beam profile with peak intensity in the centre of the beam which smoothly decreases radially outward from the centre. By properly choosing the incident laser fluence, it is possible to control only a fraction (the central peak region) of the focused Gaussian beam within which the fluence is greater than the threshold of the material, to machine. Therefore, the ablated region can be restricted to a very small area, much smaller than the diameter of the focused spot size [5, 6]. Features as small as 1/10th of the laser focus spot size has been reported and proven achievable. The principle of this technique is illustrated in Fig. 1a.

However, the sub-spot size ablation mechanism has a limit as to how small a feature it can produce, and it has reached its lowest limit when it hit the 1/10th of the laser focal spot size range. The smallest laser drilled feature reported is an amazing 200 nm in diameter [5, 7]. To break through this limit and achieve significant decrement in the feature size is currently the main challenge faced by researchers in this field.

 Fax: +65-6790-4674, E-mail: HoShookFoong@pmail.ntu.edu.sg

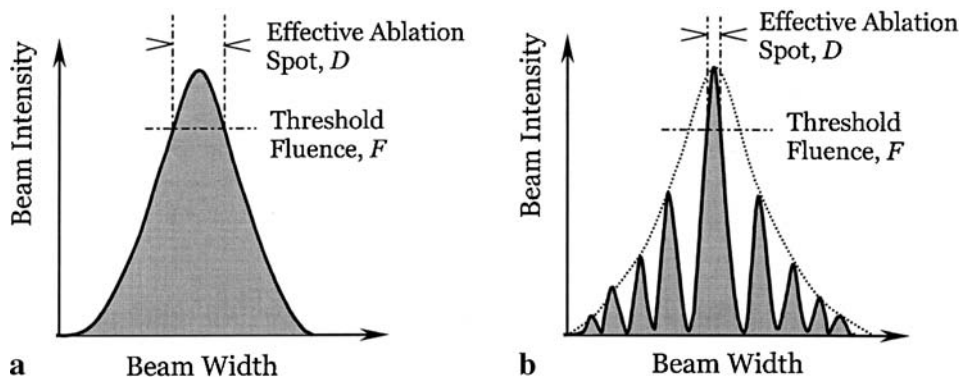


FIGURE 1 a 2D profile of the conventional non-interfered Gaussian laser beam. b 2D profile of the interfered Gaussian-like laser beam

1.2 Mechanism of sub-drilling with the interfered ultrafast laser beam

To overcome this hurdle, a novel concept of first interfering with the laser light, and then using the central bright fringe of the interfered beam to drill, thus effectively reducing the effective ablation spot size and subsequently, reducing the size of the drilled features, has been developed. The principle of this technique is illustrated in Fig. 1b.

By comparing the intensity profile of the interfered beam with the conventional non-interfered beam in Fig. 1, it is clear that by carefully controlling the threshold fluence of the laser, the interfered beam can be manipulated such that only a portion of the central fringe will machine. Therefore, the effective ablation spot of the laser can be significantly reduced, subsequently reducing the diameter of the drilled features obtained.

2 Experimental set-up

A commercial femtosecond CPA based Ti : sapphire pulse laser system (BMI Alpha-1000S) is used. The laser system comprises a Ti : sapphire oscillator, a pulse stretcher, a regenerative amplifier pumped by a Nd : YLF laser, and a pulse compressor. The system provides laser pulses at 800 nm with variable pulse output energy of up to of 800 mW or 800 μ J, and a pulse width of 150 fs at the pulse repetition rate of 1 kHz.

In order to obtain interference fringes on the ultrafast pulse laser, a Newton's Ring interferometer set-up was integrated into the experimental set-up. The schematic of the experimental set-up is shown in Fig. 2 below.

The beam wavelength from the laser system falls between 790 nm and 810 nm and is frequency centred at 800 nm in the red light spectrum region. However, most important, manu-

facturing materials such as metals, ceramics and silicon are poor absorbers of red wavelength light as compared to the ultraviolet (UV) wavelength range [7]. Therefore, for the optimisation of machining efficiency, the fundamental beam from the laser system ($\lambda = 800$ nm) is transmitted through a 0.5 mm thick non-linear SHG BBO crystal (Second Harmonic Generator) to frequency double, to generate pulses of wavelength 400 nm in the visible UV.

Gold was used for the investigation of this research work based on its wide application in the semiconductor industry for electronic packaging [8]. Pure Gold was sputtered on a 2'' \times 2'' \times 3 mm fused silica substrate to produce the 1000 \AA thick Gold film workpiece used in this experiment.

3 Theoretical analysis and visualisation using MATLAB[®]

The ultrafast pulse laser beam has a Gaussian intensity profile corresponding to the theoretical TEM₀₀ mode. The intensity distribution of the Gaussian TEM₀₀ beam is given by the term

$$I = I_0 \exp\left(-\frac{2r^2}{\omega_0^2}\right), \quad (1)$$

where, I_0 = intensity of the incident beam, r = radius of the incident beam, ω_0 = Gaussian beam radius (the radius at which the intensity has decreased to $1/e^2$ or 0.135 of its peak value).

For common optical path interferometers such as the Newton's Ring interferometer, the amplitude and intensity of both laser beams to be interfered are equal. Therefore, the interfer-

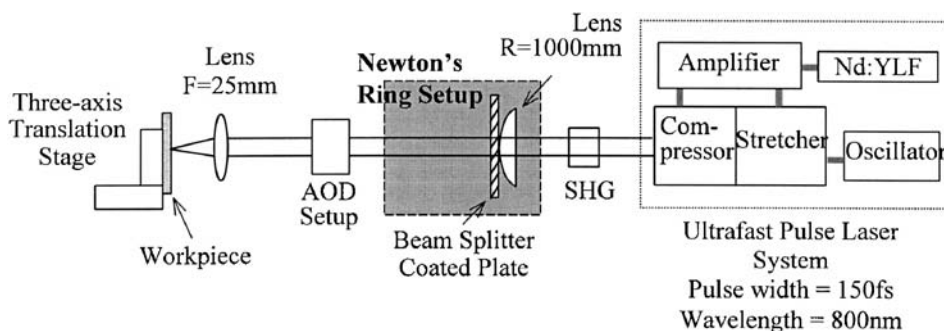


FIGURE 2 Schematic of the experimental set-up

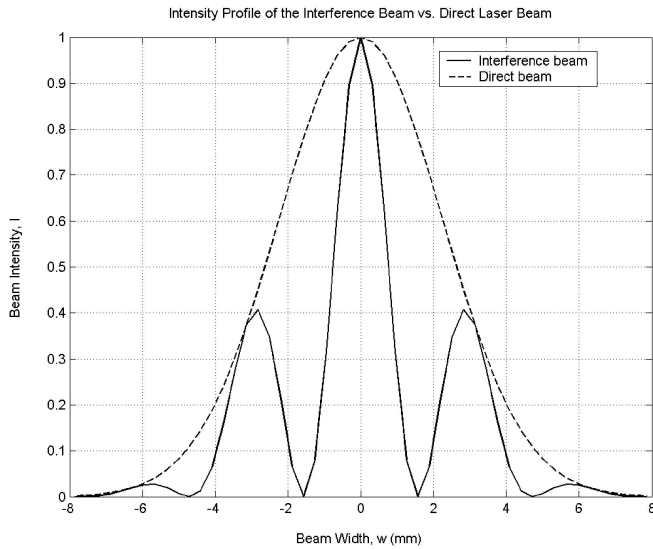


FIGURE 3 The graph plotted for the intensity profile of the direct laser beam vs. interference beam using MATLAB®

ence intensity term can be written as

$$I = 2I_0(1 + \cos \delta) = 4I_0 \cos^2 \frac{\delta}{2}, \tag{2}$$

where, I_0 = intensity of the incident beam, δ = phase difference.

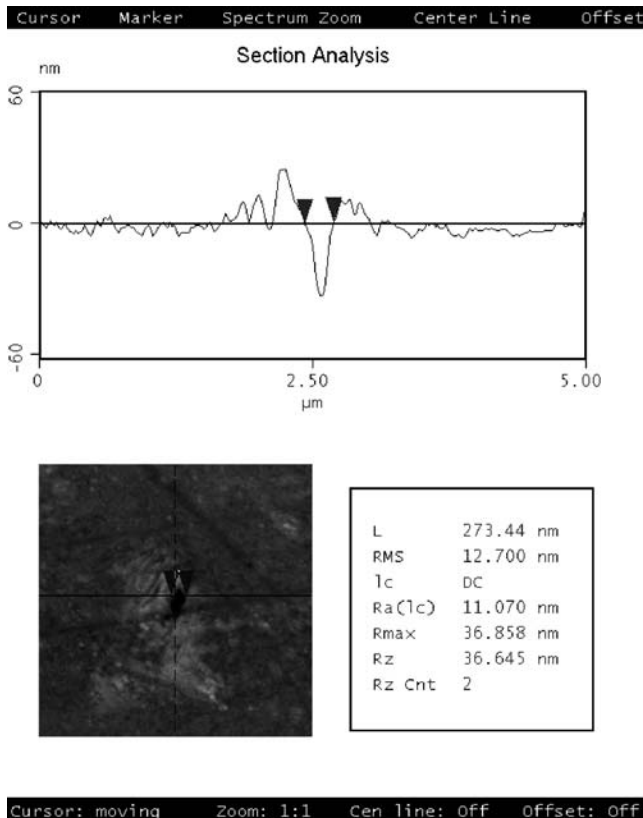
However, the above term applies only for ideal cases. Due to losses through reflection and absorption, etc, the beam will assume a gradually dissipating distribution. By using a beam analyser (BeamScope™ from DataRay Inc), it was ascertained that the interfered beam takes on a Gaussian profile. Therefore, the interference intensity function (2) is convoluted with the Gaussian distribution function to obtain the interference intensity distribution term (3)

$$I = 4I_0 \cos^2 \frac{\delta}{2} \times \exp \left(-\frac{2r^2}{\omega_0^2} \right). \tag{3}$$

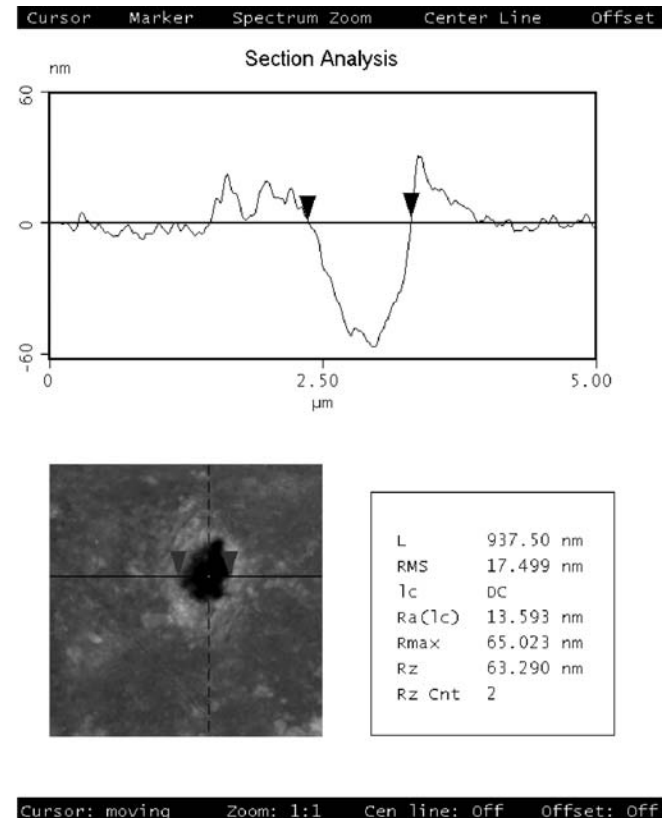
Using MATLAB®, the Gaussian beam function (1) is plotted against the interference beam function (3). The graph generated (Fig. 3) reinstates that the effective ablation spot of the laser can be significantly reduced if the laser beam is first interfered with, and then the central bright fringe used for machining as compared with just using the direct laser beam.

4 Results and discussion

The interfered laser beam from the experimental set-up in Fig. 2 is scanned across the stationary workpiece using an acousto-optic deflector (AOD) and focussing lens set-up. The Newton’s Ring set-up is then removed and the direct beam is scanned across the workpiece maintaining all machining parameters and at constant beam energy of 8 nJ. The drilled holes from both set-up configurations are then compared.



a



b

FIGURE 4 a AFM analysis on the feature drilled using the interfered laser beam. b AFM analysis on the feature drilled using the direct laser beam

An AOD is used to manipulate the laser beam to scan across the workpiece instead of using the three-axis stage to avoid problems and errors such as backlash, stick/slip effect and hysteresis which is inevitable in all mechanically driven and spring loaded equipment. As the machining features are in the sub-micron ranges, such errors are very detrimental on the machining quality, resolution, repeatability and accuracy. The role of the three-axis stage in the set-up is to ease the process of focusing the laser beam onto the workpiece for machining and to position the workpiece in between machining.

Figure 4a is the AFM analysis of the drilled feature obtained on the 1000 Å thick Gold film using the interfered laser beam while Fig. 4b is for the feature drilled using the original non-interfered laser beam. For both cases, the pulse energy used is 8 nJ.

A 285 nm ($\approx 0.3 \mu\text{m}$) hole was drilled with the interfered laser beam compared to the 950 nm ($\approx 1 \mu\text{m}$) hole using the original non-interfered laser beam at the same beam energy. This is equivalent to a 300% decrement in the drilled feature size obtained.

5 Conclusion

300 nm holes were successfully drilled on a 1000 Å thick Gold using the interfered laser beam compared to the

1 μm holes drilled using the conventional non-interfered laser beam at the same pulse energy. This is equivalent to a 300% reduction in drilled feature size, a substantial improvement in feature size obtained.

However, there is still much potential yet untapped in this research concept. For future investigation, work will be concentrated on the refinement of the interference fringes as this is the main key to achieving finer, sharper machining features with better aspect ratios.

REFERENCES

- 1 R.D. Schaeffer: Industrial Laser Solutions for Manufacturing **14**, 9 (1999)
- 2 M. Kilgo: Industrial Laser Solutions for Manufacturing **14**, 27 (1999)
- 3 T. Lizotte: Industrial Laser Solutions for Manufacturing **17**, 58 (2002)
- 4 T. Lizotte, O. Ohar: International Symposium on Flexible Circuits and Chip Scale Packaging (2003)
- 5 P.P. Pronko, S.K. Dutta, J. Squier, J.V. Rudd, D. Du, G. Mourou: Opt. Commun. **114**, 106 (1995)
- 6 B.N. Chichkov, C. Momma, S. Nolte, F.V. Alvensleben, A. Tunnermann: Appl. Phys. A: Mater. Sci. & Proc. **63**, 109 (1996)
- 7 P. Simon, J. Ihlemann: Appl. Surf. Sci. **109**, 25 (1997)
- 8 National Materials Advisory Board, Commission on Engineering and Technical Systems, National Research Council: *Materials for High-Density Electronic Packaging and Interconnection* (National Academy Press, Washington 1990)